كلية الهندسة بشبرا
FACULTY OF ENGINEERING AT SHOUBRA
ERJ
PRINT ISSN 3009-6049
ONLINE ISSN 3009-6022

**ENGINEERING RESEARCH JOURNAL (ERJ)**
Volume (54),Issue (2)
April 2025, pp:7-19
https://erjsh.journals.ekb.eg

# An Explainable model for diagnosing different grades of Brain Tumor

**Hala Badr Kamal [1,*], Lamiaa Elrefaei [1], Eman Abdel-Ghaffar [1]**

*[1] Electrical Engineering Department, Faculty of Engineering at Shoubra, Benha University, Cairo, Egypt.*
**Corresponding author*

*E-mail address: hala14833@feng.bu.edu.eg, lamia.alrefaai@feng.bu.edu.eg, eman.mohamed@feng.bu.edu.eg*

**Abstract:** A brain tumor is characterized by the uncontrolled growth of cells in the brain due to genetic mutations in the deoxyribonucleic acid (DNA) of these cells' genes. There are four grades of brain tumor develop- ment. So the doctor must detect the grade to which the patient has arrived to develop the appropriate treatment plan but this tumor grade detection process is difficult. For this reason, in this research we propose an accurate detection of brain tumor disease utilizing various deep learning and machine learning techniques. In this research two publicly available datasets used: FigShare and Rembrandt dataset. The pre-trained MobileNet model was trained on only axial magnetic resonance imaging (MRI) images from the two datasets. The pre-trained MobileNet was fine-tuned for feature extraction. Then applied ML mod- els (Random Forest, Support vector machine and Decision tree) to classify brain tumor types from the first dataset and brain tumor grades from the second dataset. Which achieved superior accuracy compared to other models 99% and 99.74% accuracy for the two datasets. To explain the results from the pre-trained MobileNet model, two types of XAI methods were applied: Grad-CAM and Shap.

**Keywords:** Brain Tumor (BT), classification, explainable artificial intelligence (XAI), Gradient-weighted class acti- vation mapping (Grad-CAM), SHapley Additive exPlanations (SHAP)..

## 1. Introduction

Brain tumor (BT) is a type of tumor that develops in the brain or central nervous system as a result of uncontrolled cell growth [1]. According to statistics from the American Society of Clinical Oncology (ASCO), the 10th most common cause of death for both men and women is cancer of the brain and nervous system. According to brain tumor statistics, tumors that metastasize to the brain affect about 25% of cancer patients, or an estimated 150,000 people annually [2]. There are many symptoms of brain cancer such as frequent headaches, difficulty in concentration, memory loss, changes in speech, loss of balance, mood swings and seizures. When a mutation occurs in DNA, this causes a malfunctioning of the genes and thus uncontrolled growth of cells which is the main cause of a tumor. The degree of mutation and the type of gene determine the grade and type of brain tumor.

There are more than 40 main types of brain tumors [3], which can be categorized in various ways based on their progression rate, growth rate, origin and nature. The benign or malignant are the main types of brain tumor. In addition, brain tumors are classified according to their origin as primary and secondary brain tumors. Based on growth rate, brain tumors are categorized by the World Health Organization (WHO) into four grades: I, II, III, and IV as shown in Figure 1 [3]. There are various factors that cause DNA mutations such as environmental factors (such as X-rays, UV light, viruses, pollution), lifestyle, and eating habits. Viruses cause approximately 15% of malignancies, but only a few have been identified, including DNA viruses and retroviruses. In the clinical examination, the neurologist in neurological exam checks patient's vision, hearing , alertness, muscle strength and reflexes.

If any symptoms of brain cancer appear, the doctor suggest one of the tests to confirm cancer depending on the patient's condition. Brain scans, tumor biopsies and biomarkers are the main tests used to identify cancer and determine its grade. Non-invasive brain scan techniques used to confirm and detect cancers include computed tomography (CT), MRI, positron emission tomography (PET) and single-photon emis- sion computerized tomography (SPECT). CT scan uses X-rays to make pictures. From Mayo Foundation for Medical Education and Research (MFMER) [4], If a patient has headaches or other symptoms that have multiple potential explanations, a CT scan may be the initial imaging test performed. The doctor may use the results as a guide to determine what tests to do next. The patient may require a brain MRI if the doctor believes that the CT scan reveals a brain tumor.

The most widely used non-invasive method for detecting abnormalities is MRI, which is safer than CT and has good contrast resolution for many tissues. This makes it easier to see smaller tumors. There are various sequences from MRI. The most frequently utilized for brain analysis are Tl-weighted, T2- weighted, and FLAIR and the basic planes of MRI are Axial, sagittal and coronal as shown in Figure 2 [1]. PET scans may be most useful for detecting quickly growing brain tumors, such as glioblastomas and some oligodendrogliomas [4]. A biopsy is an invasive removal of brain tumor tissue for laboratory examination. The appearance of cells under a microscope can indicate to the radiologist how quickly they are growing, which is referred to as the grade of the brain tumor [4]. However, it requires a

high level of experience from the radiologist because the fuzzy difference in the microscopically cell structure made it difficult to detect the brain tumor's grade. Reading brain scans or brain images to diagnose the disease depends on the proficiency of the physician, so the diagnosis may be inaccurate and may change by different observers.

Therefore, the primary aim of this study is to quickly and non-invasively determine the type and grade of the brain tumor accurately by Computer-aided Diagnostics (CAD) [5], which helps radiologists and neurologists improve the accuracy of the diagnostic results, thus saving the patient's survival. According to the ideal recommended 3T metastatic brain tumor imaging protocol in [6], radiologists can use post- contrast sagittal or axial T1 MRI images to diagnose the brain tumor. We focus on one axis in our research which is the axial axis. Explainable models use explanation methods to show why the model predicts this output [7]. There are many explanation methods that are used either within, pre-hoc or

post-hoc the model. These methods focus on domain features such as image pixels, which influence the model's output. Then these models make doctors understand how the model classifies the tumor, thus trust the model and decide to use it for accurate diagnosis. Thus, we created our models to be explicable.

Our primary objectives: Employ two data sets: FigShare and rarely used Rembrandt data. Focus on only the axial axis from MRI images of these data to make our model be not distracted and so can get a high accuracy with a little number of images compared to other researches. Pre-process the data to improve the model's training performance and reduce computation. Train the pre-trained MobileNet model for using it in two process which are classification the type and grade of the brain tumor and feature extraction. Explain how the pre-trained MobileNet learn the data using the Shap and Grad_Cam. Classify the brain tumor type and grade using three ML models (SVM, RF and DT) based on the extracted features from the pre-trained MobileNet. The rest of this article is organized as follows: Section 2 provides a review of researches that classified brain tumor grades and/or types either with XAI or not. Section 3 explains the methodology used to classify the brain tumor types using FigShare dataset and brain tumor grades using Rembrandt dataset and integrates the two XAI techniques. In section 4 we show and discuss the results of our experiment, we also demonstrate how we successfully achieved our goal. Finally, In Section 5, we summarize our efforts and discuss our future goals.

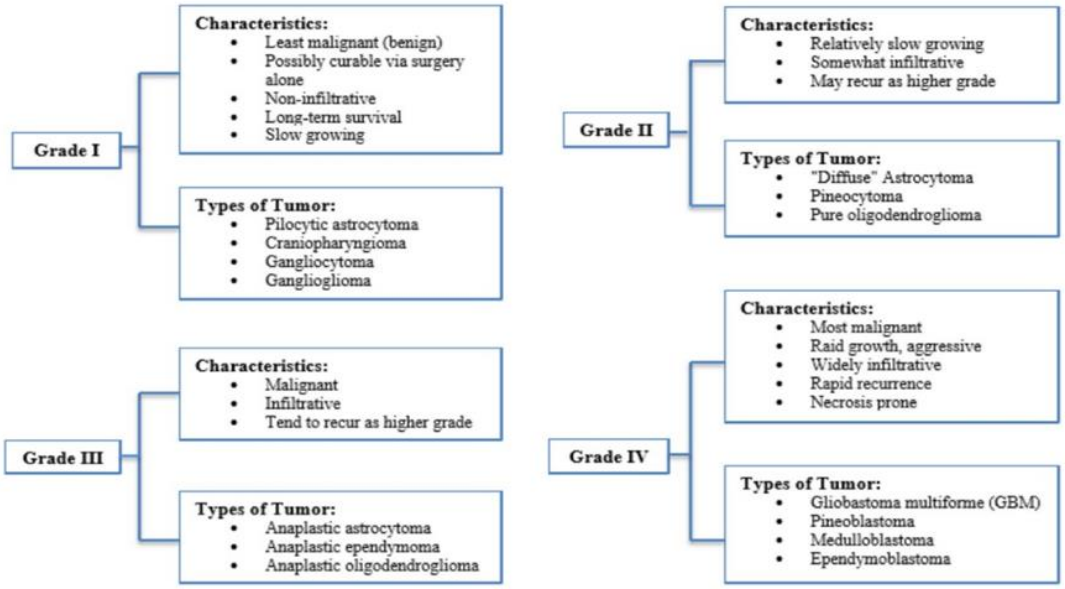


**Figure 1:** Brain tumor grades provided by WHO [3].

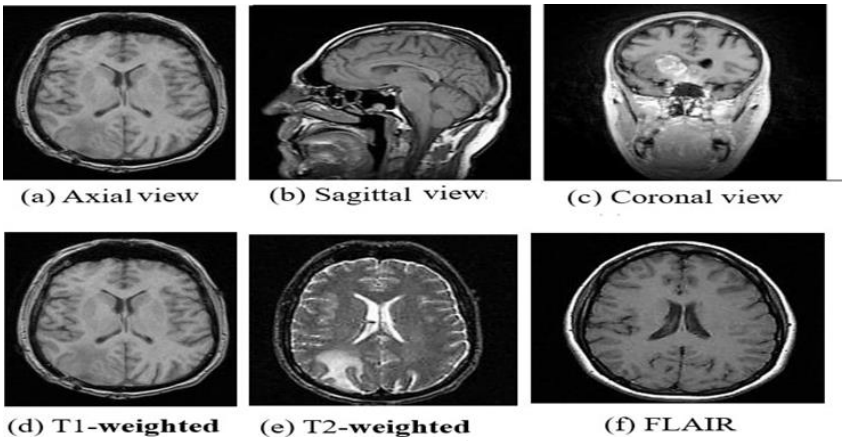


**Figure 2:** Sequences and plans of MRI tumor image [1].

## 2. RELATED WORKS

The larger number of researchers interested in classification only types of brain tumor, while little number of researchers interested in classification the grades of BT. All researches used all three axis of BT. So, this research focuses on classifying both types and grades of the only axial axis from the BT. The most significant researches in this topic will be presented in this section.

### 2.1 Classifying tumor or non-tumor

In [8] Khan et al used CNN with Adam optimizer for feature extraction and CNN with transfer learning (VGG-16, Inception-v3, ResNet50) for classification tumor and non-tumor MRI images from Kaggle. CNN model achieved the highest accuracy 100%. Seetha, J., and S. Selvakumar Raja in [9] classified MRI images from the BRATS2015 dataset into tumor or non-tumor using a pre-trained CNN model, SVM and DNN. Where the pre-trained CNN model achieved 97.5% accuracy. Tazin et al in [10] classified the X-ray images from the Kaggle dataset into healthy and brain tumor patients using transfer learning with MobileNetV2 that achieved 92% accuracy. Kumar et al in [11] used two datasets (BRATS, SimBRATS) to classify the MRI images as tumor or non-tumor. They proposed Optimization-driven deep convolution neural network for classification.

First, FCM model and deformable model are applied on the ROI (obtained from pre- processing process) for segmentation process. Then multiplied by the optimal constants generated by the Dolphin-SCA ap- proach. They used the power LBP model for feature extraction. The accuracy achieved with the BRATS dataset is 95. 3% and with the SimBRATS dataset is 96.3%. Mayar M. Alfares et al in [12] proposed a novel Distributed deep learning approach (DL). They vertically distributed Kaggle MRI images among two hospitals. The classification (healthy, tumorous) accuracy of this work is 90.688%. The downside of this strategy is that the datasets supporting vertical distribution are not publicly available and need a significant amount of resources.

In [13] Dikici, Engin and Nguyen et al achieved an accuracy of 90% in Detection of Brain Metastases using candidate detection CNN (cdCNN). In [14] Marmolejo-Saucedo et al proposed the Numerical Grad- Cam based explainable Convolutional Neural Network (numGrad-CAM-CNN) to classify MRI images (tumor, non-tumor) from the BRATS 2017 dataset. They compared various CAM methods (numGrad- CAM, Default CAM, (Default) Grad-CAM, Grad-CAM++ and Score-CAM). Physicians employed the numGrad-CAM-CNN model with 97.11% accuracy after technical and physician-oriented (human-side) evaluations. The Class Activation Mapping (CAM) approach that is employed within the developed CNN model is the XAI method in this work.

### 2.2 Classifying the types

Almalki et al in [15] extracted features from scaled and cropped MRI images using a variety of pre- trained CNN models from the kaggle dataset and various ML models (DT, NN, Naïve Bayes, KNN, ensemble, SVM) to classify the brain tumor type from four classes (meningioma, glioma, pituitary tu- mors, no tumor). Where the 22-layer CNN pre-trained model with SVM model achieved the most high accuracy(98%). In [16] Deepak et al developed three independent models with the same CNN and the same training data from FigShare but different loss function (cross entropy loss (Lce), class weighted loss (Lwce), weighted focal loss (Lwf)) to get three different feature vectors. These vectors are fused to create the fused feature vector that was used in the classification process.

The classification models are built using KNN and SVM compared to the pre-trained ResNet-18 model. Where CNN model with (Lce, Lwf) and the SVM model achieved an accuracy of 95.4%, CNN model with (Lce, Lwf) and KNN model achieved accuracy of 95.4%, pre_trained ResNet-18 model with (Lwce) and KNN model achieved accuracy of 92.5% and when using the majority voting technique on the KNN model they achieved the most high accuracy of 95.6%. Kaplan et al in [17] extracted effective features by applying Local Binary Patterns (LBP), Local binary patterns between relations between neighbors (nLBP) and local binary patterns based on angles (αLBP) to T1 weighted MRI images from (brain tumor dataset from FigShare). Then histograms of LBP, nLBP and αLBP tumor images were created.

The machine learning model uses the patterns shown in the histogram as features. The three tumor types (pituitary, glioma, and meningioma) were predicted using the KNN, ANN, RF, A1DE, LDA and SVM prediction models. Knn with nLBP (d = 1) achieved the best accuracy of 95.56%. Also, they achieved 93.50% when they used uniform pattern obtained from nLBP(d=1) with the knn classifier. When they used the selected feature approach with Knn with LBP patterns, the 92.62% accuracy is achieved. In

[18] Ismael et al classified the MRI images obtained from (brain tumor dataset from FigShare) using the pre-trained ResNet50 model. To increase the input data, they applied different augmentation techniques. The data set was then split into training and validation sets based on images and patients.

They achieved 97% accuracy at the patient level and 99% accuracy at the image level. In [19] Ghassemi et al combined OASIS data (dementia dataset) with FigShare data to train a generative adversarial net (GAN). They classified three types of brain tumors (pituitary, glioma, and meningioma) using the Pre-trained GAN discriminator (DCGAN) with only FigShare data. They applied data augmentation for pre-processing and CNN with Adam optimizer for feature extraction. They achieved with random split 95.60% accuracy. In [20] Das, Sunanda et al. used FigShare MRI images as input data to the CNN model to classify three types of brain tumors (meningioma, glioma, pituitary tumor). In pre-processing, they resized the images. Then a Gaussian filter was applied to smooth the images and histogram equalization. They proposed a CNN network structure where the features were extracted from three convolution layers and two subsampling layers with 94.39% classification accuracy.

Balaji et al in [21] compared various pre-trained CNN models (VGG16, Xception, ResNet, MobileNet, EfficientNet-B0) to classify four types of brain tumor (pituitary, glioma, meningioma, no-tumor). The highest accuracy 97.6% is achieved using the pre-trained EfficientNet-B0 model. They made Cropping and resizing the image, MR Bias Correction, Gaussian blur filter addition, BM3D_ denoised, Total variation smoothing for noise reduction, skull stripping and no-tumor images augmentation in pre-processing. Gaur et al in [22] suggested an explainable Dual-Input CNN model for classifying three types of brain tumor (pituitary, glioma, meningioma) from the kaggle dataset with accuracy of 94.64%. The XAI approaches used here are shapley additive explanation (SHAP) and local interpretable model agnostic explanations (LIME) for a simple human interpretation.

Zulfiqar et al in [23] fine-tuned five pre-trained EfficientNets (EfficientNetB0 to EfficientNetB4) models for feature extraction and classification of T1-weighted Contrast-Enhanced Magnetic Resonance Images (CEMRI) from the FigShare dataset into three classes (meningioma, glioma, pituitary tumor). Efficient- NetB2 training accuracy is 100% and the test accuracy is 98.86%. Grad-CAM is evolved for the visual representation of EfficientNetB2 predictions. Data from Kaggle is used for cross validation on external cohort with accuracy of 91.35%. In [24] Burak et al used two datasets, FigShare and Kaggle. They sug- gested SVM for classification as well as DenseNet201 and the Grad-Cam-Based Model for detecting brain tumors. They achieved 98.42% with FigShare and 99.96% with kaggle.

Atika Akter et al in [25] used six datasets. They proposed U-Net-based segmentation model and CNN model for classification. The CNN model consists of 39 layers and includes two blocks. This model used to classify the total of four individual datasets and two new merged datasets which are combinations of these datasets. First data from FigShare and second data from Kaggle. They achieved accuracy of 96.7% with FigShare, 89.4% with Kaggle and 98.7% with the merged dataset(FigShare and Kaggle). Shirin Kordnoori et al in [26] proposed a unique automatic model includes a common encoder for feature representation, one decoder for segmentation and a multi-layer perceptron. They classified three types of brain tumor from FigShare. They evaluated the output in both multi-task and single-task learning model. The multi-task learning model achieved 97%.

### 2.3 Classifying the grades

In [27] Sharif, Muhammad Irfan et al improved the contrast of MRI scans using the DHEACO approach. The features of the MRI scans were then extracted using a 9-layer CNN model. from the (BRATS 2013, BRATS 2015, BRATS 2017, BRATS 2018) datasets. Then, differential evolution (DE) and moth flame (MF) optimization algorithms were performed separately. Finally, they employed the matrix length technique to merge the two feature matrices into a single matrix. They compared various ML models (MC-SVM, Naı¨ve Bayes, Fine KNN, Decision Tree) with each of the datasets and the MC-SVM model with the BRATS 2013 dataset achieved the most high accuracy 99.06%. Gurunathan, Akila and Batri Krishnan in [28] proposed 7_layer CNN Deep net for classifying (normal, abnormal). In conjunction with the connected component method, the global thresholding strategy is used to segment tumor regions if they are abnormal.

The segmented tumor regions were diagnosed into either malignant or benign meningioma using GLCM in conjunction with a CNN classifier. The accuracy achieved from CNN Deep Net is 99.4% and from CNN-GLCM is 99.5%. The dataset used in this work is BRATS. In [29] Zeineldin et al have the primary objective which is to create a new explainability framework called NeuroXAI to provide explainable 2D and 3D sensitivity maps that will aid physicians in comprehending and applying the DL model. This work aims at classifying the HGG and LGG MRI images from the BraTS 2019 dataset by CNN network with the pre-trained ResNet-50 model with an accuracy of 98.62% and using an encoder–decoder neural network called 3D DeepSeg from BraTS 2021 to segment the glioma tumor's tumor core (TC), enhancing tumor (ET) and whole tumor (WT) regions.

NeuroXAI offers seven state-of-the-art XAI methods (XAI visualization, Vanilla gradient, guided back-propagation, integrated gradients, guided integrated gradients, SmoothGrad, Grad-CAM, guided Grad- CAM) in the classification and segmentation for both 2D and 3D medical image data that were used after the training process as post hoc XAI methods to make no retraining of the network or architecture modifications. In [30] Yan et al proposed two models which are segmentation and classification with the BraTS Challenge 2018 data set. The used pre-processing methods are z-score normalization, intensity transformation and random flip and rotation. They used VGG based on RepOptimizer for the classi- fication model with 95.46% accuracy. They generated heatmaps from the classification network using Grad-CAM++ to better display the tumor region.

In [31] Esmaeili et al retrained more than a model with three-fold cross-validation included DenseNet-121, GoogLeNet and MobileNet with TCGA dataset to classify two grades of brain tumor which is lower-grade gliomas and glioblastoma (WHO grade IV). They used N4BiasCorrection, intensity normalization and resized the MRI images to 256 × 256 × 128. They achieved 92.1% accuracy with the DenseNet-121 model. They implemented Post-hoc Grad-CAM to visualize each model's performance. Saluja et al in

[32] proposed a novel approach that integrates a customized U-Net for segmentation and VGG-16 for classification from the BraTS 2018 dataset. They used pre-processing methods in this work: gamma correction, data augmentation and normalization. The classification accuracy is 97.89%. Abd-Ellah in

[33] proposed an automatic brain-tumor diagnosis system which is TRDCNN architecture. They used a CNN for detection, classification, and segmentation of glioblastomas from BraTS 2017 dataset. TRDCNN architecture achieved 98.88% in classification process.

### 2.4 Classifying both types and grades

Rizwan et al in [34] have two purposes of their study: classify tumors into (pituitary, glioma, meningioma) using FigShare data and predict the grade of glioma (grade II, grade III, grade IV) using data from The Cancer Imaging Archive (TCIA). In pre-processing, a Gaussian filter and data augmentation are applied. Gaussian Convolution Neural Network (GCNN) is the proposed CNN network which achieved in the classification process 99.8% accuracy and in the prediction process 97.14% accuracy. Anaraki, Amin Kabir et al in [35] proposed two case studies. In Case Study I, the classified classes are Normal, Grade II, Grade III, Grade IV with 90.9% accuracy. In Case Study II, the classified classes are Glioma, Meningioma, Pituitary with accuracy of 94.2%. To find an appropriate CNN architecture for classifying MRI images, the genetic algorithm (GA) is suggested.

The best model identified by the GA was bagged to reduce the variance of classification error. Gadolinium-enhanced T1 images are used in Case Study I and II, so the tumor boundary was better determined. The datasets used in Case Study I (normal brain MRI images from the brain development website (IXI dataset), Glioma tumors from cancer imaging archive (TCIA) datasets, Rembrandt dataset (HGG, LGG), TCGA-GBM contains glioblastoma multiform brain MRI, TCGA-LGG dataset includes low grade Gliomas data and brain MRI of 60 patients were obtained from the neurosurgery section of Hazrat-e Rasool General Hospital in Tehran). The datasets used in Case Study II is the axial brain tumor images from FigShare. In [36] Sajjad et al fine-tuned the VGG-19 CNN architecture for the classification of brain tumors. In this work, two datasets are used, Radiopaedia and FigShare. Radiopaedia for classifying (grade I menigiomas, grade II,III gliomas, glioblastmoas) with a classification accuracy of 90.67%.

Brain tumor (FigShare) for classifying ( meningioma, glioma, pituitary tumor) with brain type classi- fication accuracy of 94.58%. The data augmentation methods employed in this work included various noise invariance and transformation approaches with varying parameters. In [37] Chatterjee et al used GP-UNet, GP-ReconResNet and GP-ShuffleUNet to classify two datasets which are FigShare and BraTS 2020. They achieved 95% with GP-ReconResNet and FigShare and 94% with GP-ShuffleUNet and BraTS 2020. In [38] Evgin Goceri proposed a novel network utilizing the advantages of both transformers and CNN structures. he used two dataset BraTS-2020 for glioma grading (HGG, LGG) and Kaggle for brain tumor types classification. This network achieved in glioma grading 99.21% and brain tumor classification 98.66%.

## 3. MATERIALS AND METHODS

In this section, we show the pre-processing, methodology of classification and used XAI techniques.

### 3.1 Dataset

We used two publicly available datasets in our study: FigShare and Rembrandt datasets. The first data set contains 3064 T1-weighted contrast-enhanced MRI images of three axes (axial, sagittal, coronal) for 233 patients and three types of tumor: 1426 glioma, 708 meningioma and 930 pituitary MRI images. The second data set contains 1,10064 frames of three axes (axial, sagittal, coronal) from different MRI sequences for 130 patients. We use Kaggle dataset to merge with Rembrandt dataset.

### 3.2 Pre-processing

In this subsection we will discuss the pre-processing of the datasets in detail.

#### 3.2.1 FigShare dataset

We converted the images from gray scale to RGB to make it compatible with input shape of the pre-trained MobileNet model. Where the input shape of the pre-trained MobileNet model is (image size, image size, 3). To have a grayscale image represented in three channels, the gray scale value was repeated in each RGB channel. The images are stored in MATLAB (.mat) format. The type of the images is MRI. The size of the images is 512*512. We resized the images from 512*512 to 150*150 to reduce computational cost, reducing the image size is a common procedure performed by other researches such as [20], [22] and [34]. Only axial axis images are the input data to the proposed model which are 994 MRI images(209 meningioma, 494 glioma and 291 pituitary). Before training the model on these data, we shuffled the data, then performed a 70-30 train-test split so we had 695 images for training and 299 for testing. We encoded the output labels as integers (’meningioma (1)’:0, ’glioma (2)’:1, ’pituitary tumor (3)’:2).

#### 3.2.2 Rembrandt dataset

The data collected as Digital Imaging and Communications in Medicine (DICOM) files. So we use the XnViewMP program to open these files and convert them to JPG images. So we can convert it to an array to be compatible with our model input. The format of the images is JPG. The type of the images is MRI. The size of the images is 512*512. We collected only T1 sequence MRI images for the axial axis. Our criteria for collecting data are based on choosing more than one different frame for the same patient and the same axis that has a clear tumor. We resized the images from 512*512 to 150*150 to reduce computational cost. Only axial axis images are the input data to the proposed model which are 221 MRI images(55 GBM_4, 67 ASTROCYTOMA_3 and 99 ASTROCYTOMA_2). To increase GBM_4 images, we selected the T1 MRI axial axis images from GBM_4 class from Kaggle dataset and merged it with our

GBM_4 class and performed augmentation (rotation, width_shift and height_shift) Tabel 1 represents data augmentation parameter values. Also to increase ASTROCYTOMA_3 and ASTROCYTOMA_2 and balance it with GBM_4, we used the same augmentation functions. So our data set contains 447 GBM_4 MRI images, 335 ASTROCYTOMA_3 MRI images and 495 ASTROCYTOMA_2 MRI images. Table 2 represents the data before and after augmentation. We rescaled the intensity of the images. Before training the model on these data, we shuffled the data and performed a 70-30 train-test split. We

encoded the output labels as integers ('GBM_4':0, 'ASTROCYTOMA_3':1, 'ASTROCYTOMA_2':2).

**Table 1:** The data augmentation parameter values.

| Augmentation function | Range value |
|---|---|
| Rotation | 20 |
| width shift | 0.1 |
| height shift | 0.1 |

**Table 2:** The Rembrandt data before and after augmentation.

| Classes | Before augmentation | After augmentation |
|---|---|---|
| GBM_4 | 55 | 447 |
| ASTROCYTOMA_3 | 67 | 335 |
| ASTROCYTOMA_2 | 99 | 495 |
| Total | 221 | 1277 |

### 3.3 Methodology

There are many CNN models used in the image classification method, such as the MobileNet model which is trained on a large dataset which is the ImageNet dataset [39]. As shown in Figure 3 we fine-tuned the pre-trained MobileNet to use it in two strategy. First we used pre-trained MobileNet as classifier. Second we use it as feature extractor to extract features from FigShare and Rembrandt datasets, then we used SVM, RF and DT machine learning techniques to classify brain tumor types and grades from FigShare and Rembrandt datasets.

#### 3.3.1 Pre-trained Model (MobileNet)

MobileNet is the first mobile computer vision model [39]. It is a lightweight deep neural network because of the use of depthwise separable convolutions which significantly reduce the number of parameters compared to other networks [39] then it has lower complexity and higher performance than other networks, so we used it in this experiment. The first layers which extracted features in the model include Depthwise Conv2D and Pointwise Conv2D layers followed by batch normalization and the ReLU activation function at the back of each convolution layer [39]. We removed The final layers which make classification and add GlobalAveragePooling2D layer to make the dimensionality reduction, dropout layer to make regularization and prevent overfitting and dense layer to perform the classification output of three classes.

#### 3.3.2 Transfer Learning from MobileNet

We fine tuned the pre-trained MobileNet model for feature extraction as well as classification. The Mo- bileNet has 89 layers in total, the first 86 layers are used for extracting features, while the final three layers are used for classifying the features into 1,000 classes. Therefore, these final layers were removed to transfer the layers to our classification task, and then a new dropout layer and a dense layer with the softmax activation function with three classes were added. We added the GlobalAveragePooling2D layer to make the dimensionality reduction. Additionally, we employed the categorical cross-entropy loss function and the Adam optimizer. We used our data sets to retrain the model.

#### 3.3.3 Pre-trained MobileNet as Feature extractor

In this approach, we also used pre-trained MobileNet as feature extractor and three machine learning techniques SVM, RF and DT for the classification task with FigShare and Rembrandt datasets as shown in Figure 4 . We retrained the model on the input data and removed the classification layer then extracted features from the dropout layer to obtain a 1024-dimensional feature vector. Then, the classifiers are employed to perform classification task. We visualized the features maps from various layers of the pre- trained MobileNet model to show how it learns the data as the model became deeper. As shown in Figure 5 the features maps of the first layers represent the basic patterns from the input MRI image which are the low-level features like textures and edges. The features represent the more complex patterns from the input MRI image, which are the high-level features, as we move up the network layers, as shown in Figures 5 and 6. So, when the network goes deeper and deeper, it will learn more and more about the data and predict the output with higher accuracy. So we get the features from the last layer to make it the input to the classification network to achieve higher accuracy from the classifier.

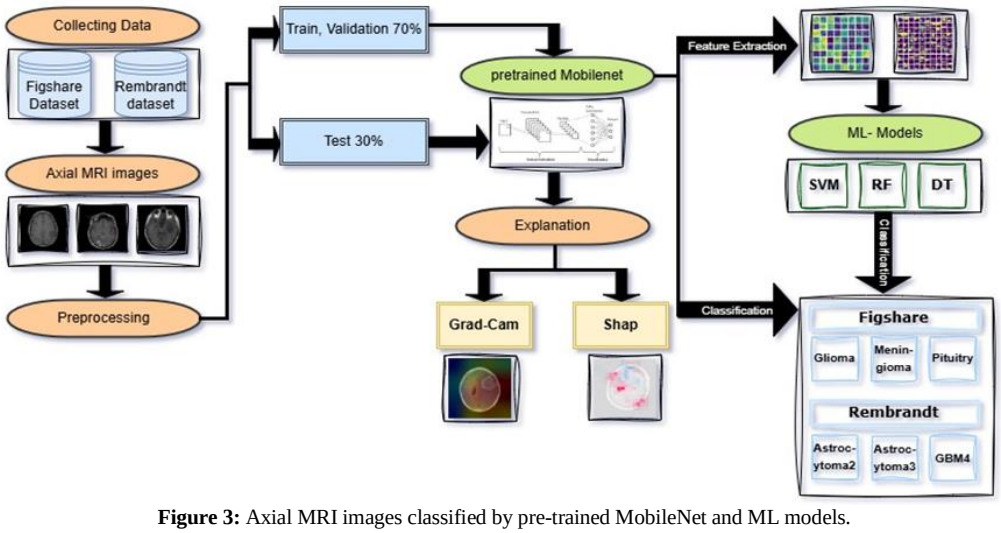


**Figure 3:** Axial MRI images classified by pre-trained MobileNet and ML models.

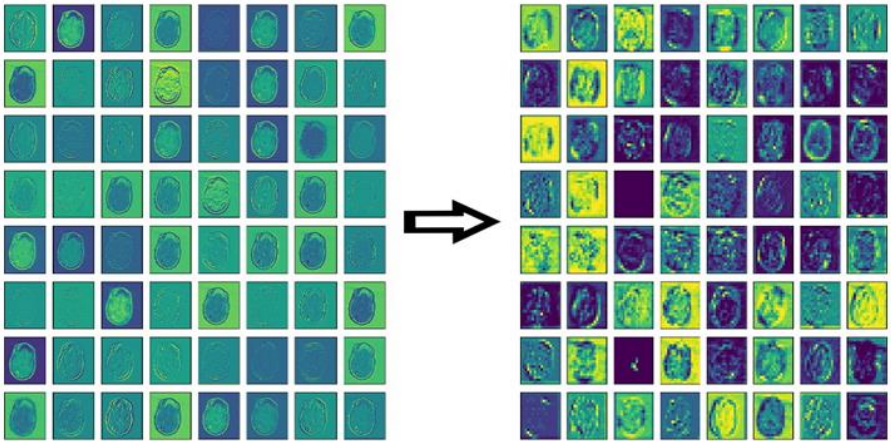

**Figure 4:** Feature maps from conv_pw_1 and conv_dw_2 layers (first layers).

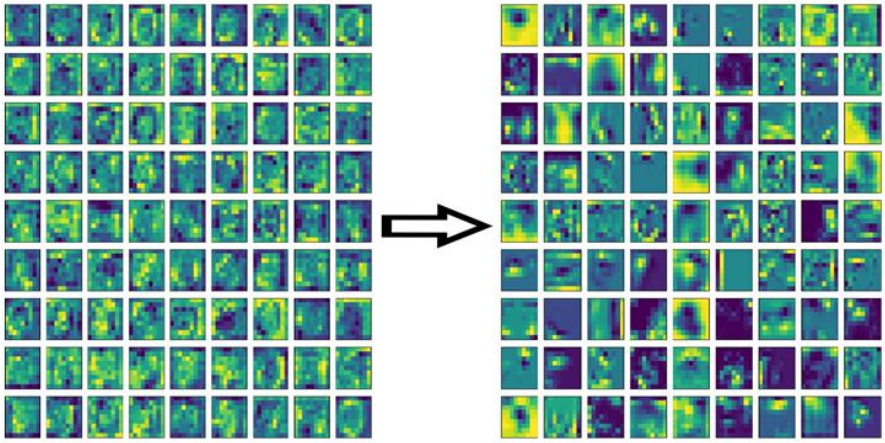

**Figure 5:** Feature maps from conv_pw_6 and conv_dw_10 layers (middle layers).

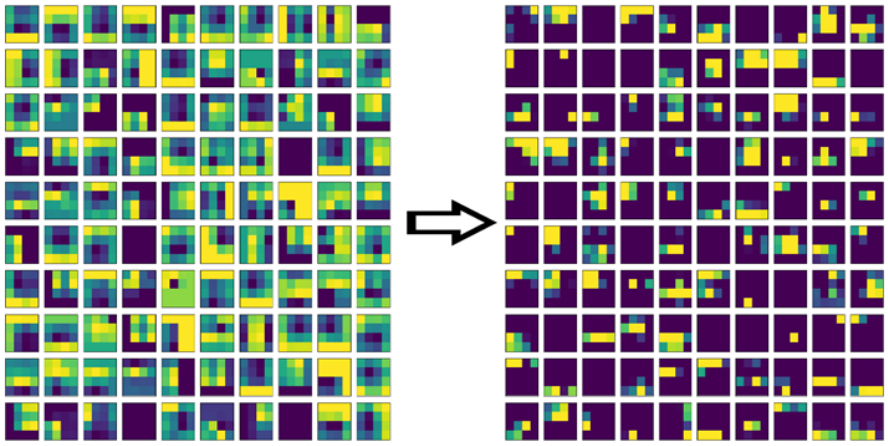

**Figure 6:** Feature maps from conv_dw_13 and conv_pw_13_relu layers (last layers).

### 3.3.4 Classification

We used three machine learning models to classify the two mentioned datasets by the features maps from the pre-trained model. We executed Support vector machine(SVM) with the popular kernel function which is the radial basis function kernel(RBF), Random Forest(RF) and Decision Tree(DT).

### 3.3.5 Explainable AI (XAI)

We applied two XAI techniques to understand how the pre-trained MobileNet model learns the data and takes its decision to predict the output. The two XAI techniques are Gradient Weighted Class Activation Mapping (Grad-CAM) applied on MRI images to show how the MobileNet learns the data during the layers of the model and Shapley Additive exPlanations (Shap) to show how features effects on the prediction. So, when using these XAI techniques, the radiologist will trust in the results of the model. Grad-CAM and SHAP have a different presentation for explanation but both highlight the same region which is a brain tumor (the model classify it).

## 4. RESULTS AND DISCUSSION

In this section, we present the results of our experiments. We conducted our experiments on 'Google- Colab', utilizing the provided GPU. The classification metrics used to evaluate the model include train and test accuracy and micro-average (precision, recall, F1 score and ROC AUC).

### 4.1 Transfer Learning from MobileNet

After pre-processing the only Axial_T1 images and splitting the datasets to train and test, we retrain the pre-trained model on the data from the FigShare and Rembrandt datasets independently. We discovered that the highest accuracy was achieved when we set the batch size to 32. Table 3 represents the training parameter values. The classification accuracy achieved using this method was 97.32% on Axial_T1 images from FigShare after 20 epocs, 96.35% on Axial_T1 images from Rembrandt after 20 epocs. Table 4 represents the results of the transfer learning model on the above mentioned datasets using metrics such as accuracy recall, precision, f1-scores and ROC AUC .

**Table 3:** The training parameter values.

| parameter | value |
|---|---|
| Dropout ratio | 0.5 |
| Dense activation | softmax |
| Batch size | 32 |
| Learning rate | 0.001 |
| optimizer | Adam |

**Table 4:** The results of transfer learning MobileNet on the FigShare and Rembrandt datasets.

| Metrics | Axial_FigShare | Axial_Rembrandt |
|---|---|---|
| Train accuracy | 99.86% | 99.58% |
| Test Accuracy | 97.32% | 96.35% |
| Precision | 97.32% | 96.35% |
| Recall | 97.32% | 96.35% |
| F1 Score | 97.32% | 96.35% |
| ROC AUC | 99.77% | 99.66% |

### 4.2 Pre-trained MobileNet with machine learning techniques

After we extracted the features from only Axial_T1 images from FigShare and Rembrandt datasets using pre-trained MobileNet model, the SVM, RF and DT classifiers used to perform the classification operation. Our experiment with the three classifier achieved 98.99%, 99% and 96.32% with FigShare and 99.74%,99.48% and 98.18% with Rembrandt. we evaluated the classifiers by 5_fold cross-validation. Table 5 and 6 represent the accuracy and validation and other metrics of the three machine learning models with the Axial_FigShare and Axial_Rembrandt datasets respectively. Figure 7 represents the confusion metrics of the SVM, RF and DT classifiers with two datasets.

### 4.3 Grad_CAM

Grad_CAM technique is one of the most popular XAI techniques used to understand how CNN models work. Grad_CAM visualizes which area is the most affected in the prediction. Grad_CAM can find the most significant parts of the input image by obtaining the gradient of the convolution layer [40] then overlapped in this image to get the heatmap showing the most and lowest significant areas for the prediction with coloration from blue which is low significant, to red which is high significant. Figure 8 shows how the pre-trained MobileNet model learns the input Axial MRI image from FigShare data across some of the model layers starting from the earlier layers (top left) to the later layers (bottom right). This shows that the model learns more features and becomes more accurate while moving on during the layers.

**Table 5:** The results of the three machine learning models on the FigShare dataset.

| Metrics | SVM | RF | DT |
|---|---|---|---|
| Train accuracy | 98.75% | 98.89% | 97.07% |
| Test Accuracy | 98.99% | 99% | 96.32% |
| validation on test data | 98.54% | 98.99% | 95.32% |
| precision | 99% | 99% | 96.32% |
| Recall | 99% | 99% | 96.32% |
| F1 Score | 99% | 99% | 96.32% |
| ROC AUC | 99.93% | 99.94% | 97.24% |

**Table 6:** The results of the three machine learning models on the Rembrandt dataset.

| Metrics | SVM | RF | DT |
|---|---|---|---|
| Train accuracy | 99.33% | 98.95% | 96.42% |
| Test Accuracy | 99.74% | 99.48% | 98.18% |
| validation on test data | 99.05% | 99.30% | 94.79% |
| precision | 99.74% | 99.48% | 98.18% |
| Recall | 99.74% | 99.48% | 98.18% |
| F1 Score | 99.74% | 99.48% | 98.18% |
| ROC AUC | 100% | 99.99% | 98.63% |

### 4.4 Shap

We used Shap with the pre-trained MobileNet model on Rembrandt dataset to compute the Shap values which show which features the model focuses on and effect more on the classification output. Figure 9 represents the Shap values that show which features the model based on to classify the MRI image with three different evaluations of the model to estimate the Shap values. When the evaluation value increased, the image became more explicable.

### 4.5 Discussion

We succeeded in achieving our aim of classifying brain tumor types and grades by only the axial planes of MRI images. The proposed model was trained on only axial MRI images from the FigShare and Rembrandt datasets individually to make the model focus on one plane during the training operation until it could classify more accurately than when training on all three planes. The pre-trained MobileNet model was fine-tuned to use it in two operations.

First, the pre-trained MobileNet model was re-trained on the FigShare data to classify the brain tumor type for the three types which achieved 97.32% test accuracy and Rembrandt data to classify brain tumor grade from three grades that achieved 96.35% test accuracy. Second, the classification layer was removed from the pre-trained MobileNet model to use it as a feature extractor. We got the features from the last convolution layer which learned more data than the previous layers as shown in Figures 4, 5 and 6.

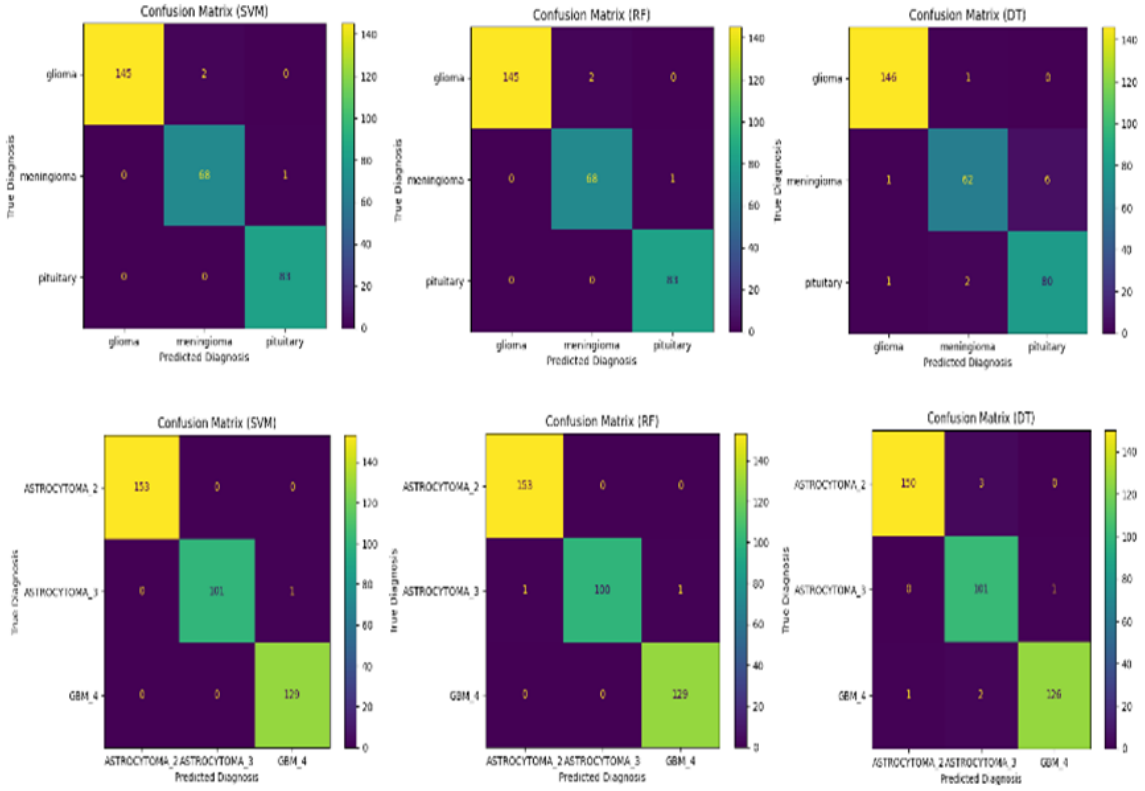


**Figure 7:** Confusion metrics of the SVM, RF and DT classifiers with the FigShare (Upper row) and Rembrandt datasets (Lower row).

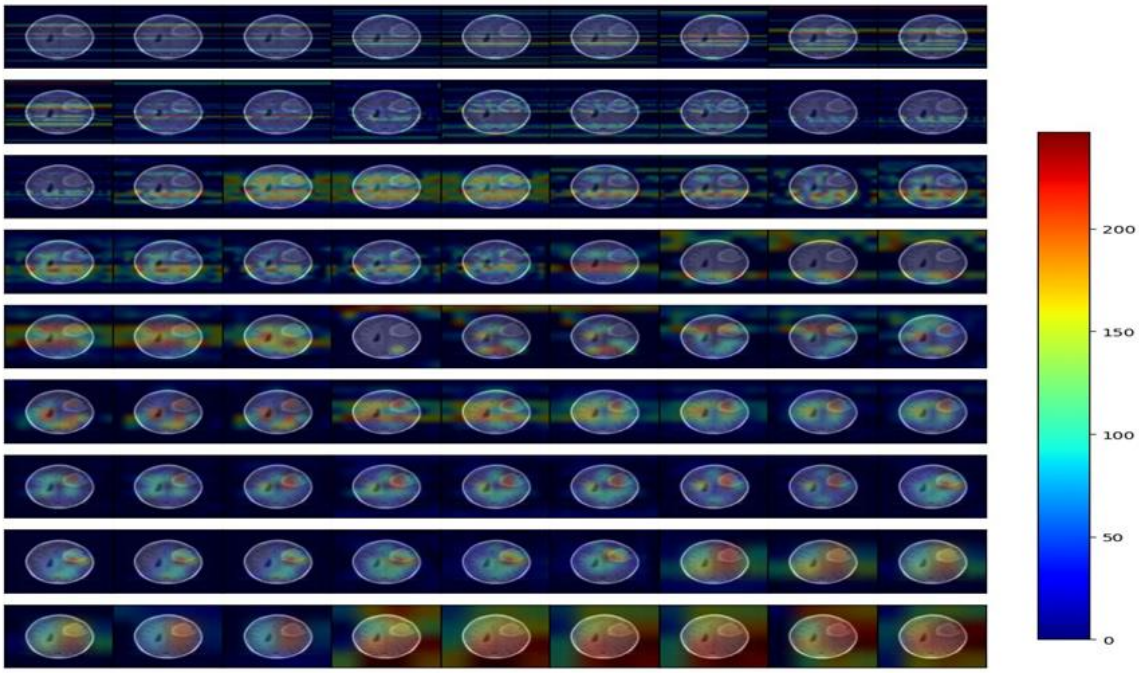


**Figure 8:** Grad_CAM for an input image from FigShare dataset during set of layers of pre- trained MobileNet.

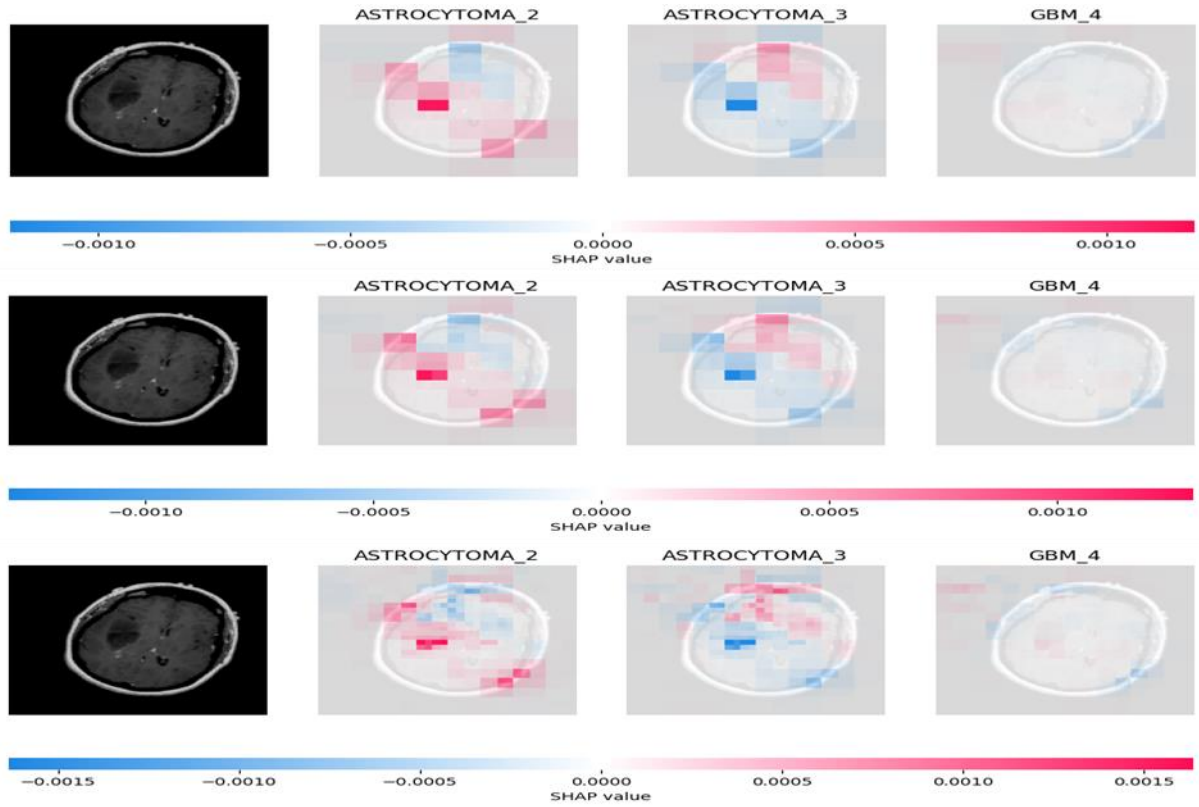


**Figure 9:** Shap values with 500, 1000 and 10000 evaluations from Top to bottom.

Which are a visualization of the features maps from various layers of the pre-trained MobileNet model to show that the model will learn more and more about the data when it goes deeper and deeper. Then we used the machine learning models with these features to classify the types of tumor from FigShare dataset and grades of tumor from Rembrandt datasets individually. We used three machine learning models in the classification process which are SVM, RF and DT which achieved 98.99%, 99% and 96.32% test accuracy respectively with the Figshare dataset and 99.74%, 99.48% and 98.18% test accuracy respectively with the Rembrandt dataset. The confusion metrics of the three machine learning models with the two datasets are computed as shown in Figure 7 to visualize the performance of these models. We also performed 5-fold cross-validation to make sure that our models did not overfit.

The train, cross-validation and test accuracy of the three machine learning models SVM, RF and DT for the two data sets are presented in Figure 10. The pre-trained MobileNet model was explained by two XAI methods: Grad_CAM in the case of FigShare data and Shap in the case of Rembrandt data to make the radiologists trust in the prediction of the model. Grad_CAM can visualize the area that is the most affected in the prediction of the model and highlighted it in a red color as shown in Figure 8 in which the tumor region highlighted in a red color. Shap represents the Shap values that show the features the model based on to classify the MRI image as shown in Figure 9 which show the shap values in three different evaluations of the model. As shown in Tables 7 and 8 the RF with FigShare dataset and the SVM with Rembrandt dataset with little data achieved a higher accuracy than other models with more data in the literature reviews.

## 5. CONCLUSION

In our study, two publicly available data sets were used which are FigShare and Rembrandt then we choose only axial MRI images in order not to distract our model, so it is more accurate with fewer number of images in comparison to other published researches. The pre-trained MobileNet model was fine-tuned and trained on the axial MRI images from these datasets individually after pre-processing these images. The pre-trained MobileNet model was used in two ways once as a classifier and in the second as a feature extractor. The classification layer was removed then the features were extracted from the last convolution layer. Then we feed these extracted features into the three ML models which are SVM, RF and DT which used in our methodology to classify the brain tumor types and grades from the two datasets. Two XAI methods (Grad-CAM and Shap) were used to explain how the pre-trained MobileNet model learn theinput data from the FigShare and Rembrandt datasets respectively.

In future, we aspire to develop a completed 3D system which can take the 3D brain MRI and cut it into the three axes axial, sagittal and coronol. Then segment the tumor and so classify the type and grade of the brain tumor. Also, making this system capable of writing the report as the radiologist does. We will collect 3D data and improve our model to handle these data and train on them. We will use more XAI methods to explain our model and make it trusted.

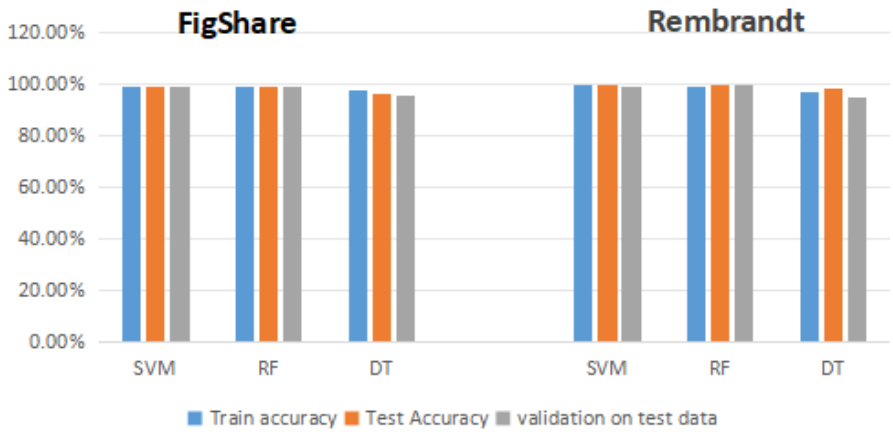


**Figure 10:** Train, cross validation and test accuracy of the SVM, RF and DT for the FigShare and Rembrandt data sets.

**Table 7:** Comparison between other researches in literature reviews that classified the types of brain tumor used FigShare dataset

| Paper | planes | Model | Accuracy | F1 Score | Recall | precision | XAI Method |
|---|---|---|---|---|---|---|---|
| [16] | All | Majority voting on KNN models | 95.6% | 94.7% | 94.4% | 95% | - |
| [17] | All | Knn with nLBP (d = 1) | 95.56% | 91.8% | 91.7% | 92.5% | - |
| [19] | All | DCGAN | 95.60% | 95.10% | - | 95.29% | - |
| [23] | All | EfficientNetB2 | 98.86% | 98.71% | 98.77% | 98.65% | Grad-CAM |
| [35] | Axial | various CNN are evolved using genetic algorithm | 94.2% | - | - | - | - |
| [36] | All | VGG-19 | 94.58% | - | 88.41% | - | - |
| [37] | All | GP-ReconResNet | 95% | 95% | 95% | 96% | - |
| [25] | All | CNN model | 96.7% | 96.7% | 93.6% | 100% | - |
| [26] | All | multi-task learning model | 97% | - | - | - | - |
| our pro-posed model | Axial | Mobilenet with RF | 99% | 99% | 99% | 99% | Grad-CAM |

**Table 8:** Comparison between other researches in literature reviews that classified the brain tumor grades using Rembrandt and other datasets

| Paper | Dataset | axis | Gades | Model | Accuracy | F1 Score | Recall | precision | XAI Method |
|---|---|---|---|---|---|---|---|---|---|
| [27] | BRATS 2013 | All | LGG,HGG | MC-SVM | 99.06% | - | - | - | - |
| [28] | BRATS | All | malignant, benign | CNN- GLCM | 99.5% | 98.1% | - | 97.6% | - |
| [29] | BraTS 2019 | All | LGG,HGG | pre trained ResNet-50 | 98.62% | - | - | - | seven XAI meth-ods |
| [30] | BraTS Challenge 2018 | All | LGG,HGG | VGG based on RepOp-timizer | 95.46% | 90.73% | - | 94.66% | Grad-CAM++ |
| [31] | TCGA | All | lower- grade gliomas and glioblas- tom | DenseNet-121 | 92.1% | - | - | - | Post-hoc Grad-CAM |

| | | | | | | | | | |
|---|---|---|---|---|---|---|---|---|---|
| [32] | BraTS 2018 | All | HGG LGG | VGG-16 | 97.89% | - | 97.50% | - | - |
| [33] | BraTS 2017 | All | HGG LGG | TRDCNN | 98.88% | - | - | - | - |
| [34] | TCIA | All | grades 2,3 and 4 of glioma | GCNN | 97.14% | - | - | 98.3% | - |
| [35] | Rembrandt and oth- ers | All | Normal and grades 2,3 and 4 of glioma | various CNN are evolved us- ing genetic algorithm | 90.9% | - | - | - | - |
| [36] | Radio- paedia | All | Grade 1 Meni- giomas, Grade 2,3 Gliomas and GBM4 | VGG-19 | 90.67% | - | - | - | - |
| [37] | BraTS 2020 | All | LGG,HGG | GP- ShuffleUNet | 94% | 0.93% | 0.94% | 0.94% | - |
| [38] | BraTS 2020 | All | HGG LGG | CNN | 99.21% | 98.74% | - | 99.22% | - |
| our pro- posed model | Rembrandt | Axial | Astrocytoma 2,3 and GBM4 | Mobilenet with SVM | 99.74% | 99.74% | 99.74% | 99.74% | Shap |

## REFERENCES


[1] Gopal S Tandel, Mainak Biswas, Omprakash G Kakde, Ashish Tiwari, Harman S Suri, Monica Turk, John R Laird, Christopher K Asare, Annabel A Ankrah, NN Khanna, et al. A review on a deep learning perspective in brain cancer classification. Cancers, 11(1):111, 2019.

[2] Key statistics for brain and spinal cord tumors. https://www.cancer.org/cancer/types/brain-spinal- cord-tumors-adults/about/key-statistics.html. [accessed on 20 April 2023].

[3] Arti Tiwari, Shilpa Srivastava, and Millie Pant. Brain tumor segmentation and classification from magnetic resonance images: Review of selected methods from 2014 to 2019. Pattern recognition letters, 131:244–260, 2020.

[4] Brain tumor - Diagnosis and treatment - Mayo Clinic — mayoclinic.org. https://www.mayoclinic. org/diseases-conditions/brain-tumor/diagnosis-treatment/drc-20350088. [Accessed 1-01-2025].

[5] Geethu Mohan and M Monica Subashini. Mri based medical image analysis: Survey on brain tumor grade classification. Biomedical Signal Processing and Control, 39:139–161, 2018.

[6] Smits M. Boxerman J. Huang R. Barboriak D. P. Weller M. Chung C. Tsien C. Brown P. D. Shankar L. Galanis E. Gerstner E. Van Den Bent M. J. Burns T. C. Parney I. F. Dunn G. Brastianos P. K. Lin N. U. Wen P. Y. Ellingson B. M Kaufmann, T. J. Consensus recommendations for a standardized brain tumor imaging protocol for clinical trials in brain metastases. https://academic.oup.com/ neuro-oncology/article/22/6/757/5734626, 2020. [Accessed 17-11-2024].

[7] Amitojdeep Singh, Sourya Sengupta, and Vasudevan Lakshminarayanan. Explainable deep learning models in medical image analysis. Journal of imaging, 6(6):52, 2020.

[8] Hassan Ali Khan, Wu Jue, Muhammad Mushtaq, and Muhammad Umer Mushtaq. Brain tumor classification in mri image using convolutional neural network. Mathematical Biosciences and Engi- neering, 2021.

[9] J Seetha and S Selvakumar Raja. Brain tumor classification using convolutional neural networks. Biomedical & Pharmacology Journal, 11(3):1457, 2018.

[10] Tahia Tazin, Sraboni Sarker, Punit Gupta, Fozayel Ibn Ayaz, Sumaia Islam, Mohammad Moniruj- jaman Khan, Sami Bourouis, Sahar Ahmed Idris, and Hammam Alshazly. [retracted] a robust and novel approach for brain tumor classification using convolutional neural network. Computational Intelligence and Neuroscience, 2021(1):2392395, 2021.

[11] Sharan Kumar and Dattatreya P Mankame. Optimization driven deep convolution neural network for brain tumor classification. Biocybernetics and Biomedical Engineering, 40(3):1190–1204, 2020.

[12] Omar S Ads, Mayar M Alfares, and Mohammed A-M Salem. Multi-limb split learning for tumor classification on vertically distributed data. In 2021 Tenth International Conference on Intelligent Computing and Information Systems (ICICIS), pages 88–92. IEEE, 2021.

[13] Engin Dikici, Xuan V Nguyen, Matthew Bigelow, and Luciano M Prevedello. Augmented networks for faster brain metastases detection in t1-weighted contrast-enhanced 3d mri. Computerized Medical Imaging and Graphics, 98:102059, 2022.

[14] Jose Antonio Marmolejo-Saucedo and Utku Kose. Numerical grad-cam based explainable convolu- tional neural network for brain tumor diagnosis. Mobile Networks and Applications, 29(1):109–118, 2024.

[15] Yassir Edrees Almalki, Muhammad Umair Ali, Karam Dad Kallu, Manzar Masud, Amad Zafar, Sharifa Khalid Alduraibi, Muhammad Irfan, Mohammad Abd Alkhalik Basha, Hassan A Alshamrani, Alaa Khalid Alduraibi, et al. Isolated convolutional-neural-network-based deep-feature extraction for brain tumor classification using shallow classifier. Diagnostics, 12(8):1793, 2022.

[16] S Deepak and PM Ameer. Brain tumor categorization from imbalanced mri dataset using weighted loss and deep feature fusion. Neurocomputing, 520:94–102, 2023.

[17] Kaplan Kaplan, Yılmaz Kaya, Melih Kuncan, and H Metin Ertunç. Brain tumor classification using modified local binary patterns (lbp) feature extraction methods. Medical hypotheses, 139:109696, 2020.

[18] Sarah Ali Abdelaziz Ismael, Ammar Mohammed, and Hesham Hefny. An enhanced deep learning approach for brain cancer mri images classification using residual networks. Artificial intelligence in medicine, 102:101779, 2020.

[19] Navid Ghassemi, Afshin Shoeibi, and Modjtaba Rouhani. Deep neural network with generative adversarial networks pre-training for brain tumor classification based on mr images. Biomedical Signal Processing and Control, 57:101678, 2020.

[20] Sunanda Das, O. F. M. Riaz Rahman Aranya, and Nishat Nayla Labiba. Brain tumor classification using convolutional neural network. In 2019 1st International Conference on Advances in Science, Engineering and Robotics Technology (ICASERT), pages 1–5, 2019.

[21] Gopinath Balaji, Ranit Sen, and Harsh Kirty. Detection and classification of brain tumors using deep convolutional neural networks. arXiv preprint arXiv:2208.13264, 2022.

[22] Loveleen Gaur, Mohan Bhandari, Tanvi Razdan, Saurav Mallik, and Zhongming Zhao. Explanation- driven deep learning model for prediction of brain tumour status using mri image data. Frontiers in genetics, 13:822666, 2022.

[23] Fatima Zulfiqar, Usama Ijaz Bajwa, and Yasar Mehmood. Multi-class classification of brain tumor types from mr images using efficientnets. Biomedical Signal Processing and Control, 84:104777, 2023.

[24] Burak Taşcı. Attention deep feature extraction from brain mris in explainable mode: Dgxainet. Diagnostics, 13(5):859, 2023.

[25] Atika Akter, Nazeela Nosheen, Sabbir Ahmed, Mariom Hossain, Mohammad Abu Yousuf, Moham- mad Ali Abdullah Almoyad, Khondokar Fida Hasan, and Mohammad Ali Moni. Robust clinical applicable cnn and u-net based algorithm for mri classification and segmentation for brain tumor. Expert Systems with Applications, 238:122347, 2024.

[26] Shirin Kordnoori, Maliheh Sabeti, Mohammad Hossein Shakoor, and Ehsan Moradi. Deep multi-task learning structure for segmentation and classification of supratentorial brain tumors in mr images. Interdisciplinary Neurosurgery, 36:101931, 2024.

[27] Muhammad Irfan Sharif, Jian Ping Li, Muhammad Attique Khan, Seifedine Kadry, and Usman Tariq. M3btcnet: multi model brain tumor classification using metaheuristic deep neural network features optimization. Neural Computing and Applications, 36(1):95–110, 2024.

[28] Akila Gurunathan and Batri Krishnan. A hybrid cnn-glcm classifier for detection and grade classi- fication of brain tumor. Brain Imaging and Behavior, 16(3):1410–1427, 2022.

[29] Ramy A Zeineldin, Mohamed E Karar, Ziad Elshaer, • Jan Coburger, Christian R Wirtz, Oliver Burgert, and Franziska Mathis-Ullrich. Explainability of deep neural networks for mri analysis of brain tumors. International journal of computer assisted radiology and surgery, 17(9):1673–1683, 2022.

[30] Fei Yan, Yunqing Chen, Yiwen Xia, Zhiliang Wang, and Ruoxiu Xiao. An explainable brain tumor detection framework for mri analysis. Applied Sciences, 13(6):3438, 2023.

[31] Morteza Esmaeili, Riyas Vettukattil, Hasan Banitalebi, Nina R Krogh, and Jonn Terje Geitung. Explainable artificial intelligence for human-machine interaction in brain tumor localization. Journal of personalized medicine, 11(11):1213, 2021.

[32] Sonam Saluja, Munesh Chandra Trivedi, and Shiv S Sarangdevot. Advancing glioma diagnosis: Integrating custom u-net and vgg-16 for improved grading in mr imaging. Mathematical Biosciences and Engineering, 21(3):4328–4350, 2024.

[33] Mahmoud Khaled Abd-Ellah, Ali Ismail Awad, Ashraf AM Khalaf, and Amira Mofreh Ibraheem. Automatic brain-tumor diagnosis using cascaded deep convolutional neural networks with symmetric u-net and asymmetric residual-blocks. Scientific reports, 14(1):9501, 2024.

[34] Muhammad Rizwan, Aysha Shabbir, Abdul Rehman Javed, Maryam Shabbir, Thar Baker, and Dhiya Al-Jumeily Obe. Brain tumor and glioma grade classification using gaussian convolutional neural network. IEEE Access, 10:29731–29740, 2022.

[35] Amin Kabir Anaraki, Moosa Ayati, and Foad Kazemi. Magnetic resonance imaging-based brain tumor grades classification and grading via convolutional neural networks and genetic algorithms. biocybernetics and biomedical engineering, 39(1):63–74, 2019.

[36] Muhammad Sajjad, Salman Khan, Khan Muhammad, Wanqing Wu, Amin Ullah, and Sung Wook Baik. Multi-grade brain tumor classification using deep cnn with extensive data augmentation. Journal of computational science, 30:174–182, 2019.

[37] Soumick Chatterjee, Hadya Yassin, Florian Dubost, Andreas Nürnberger, and Oliver Speck. Weakly- supervised segmentation using inherently-explainable classification models and their application to brain tumour classification. arXiv preprint arXiv:2206.05148, 2022.

[38] Evgin Goceri. An efficient network with cnn and transformer blocks for glioma grading and brain tumor classification from mris. Expert Systems with Applications, 268:126290, 2025.

[39] Andrew G Howard. Mobilenets: Efficient convolutional neural networks for mobile vision applica- tions. arXiv preprint arXiv:1704.04861, 2017.

[40] Khalid M Hosny, Mahmoud A Mohammed, Rania A Salama, and Ahmed M Elshewey. Explainable ensemble deep learning-based model for brain tumor detection and classification. Neural Computing and Applications, pages 1–18, 2024.